

RECENT ADVANCES IN DIRECT-DRIVE ICF TARGET PHYSICS AT THE LABORATORY FOR LASER ENERGETICS

R. L. MCCRORY, J. M. SOURES, A. BABUSHKIN, R. E. BAHR, R. BETTI, T. R. BOEHLY, R. BONI, D. K. BRADLEY, T. J. B. COLLINS, R. S. CRAXTON, J. D. DELETTREZ, W. R. DONALDSON, R. EPSTEIN, V. YU. GLEBOV, V. N. GONCHAROV, R. Q. GRAM, D. R. HARDING, D. G. HICKS,** B. HUGHES, P. A. JAANIMAGI, T. J. KESSLER, J. P. KNAUER, C.K. LI,** S. J. LOUCKS, F. J. MARSHALL, P. W. MCKENTY, D. D. MEYERHOFER, A. V. OKISHEV, S. PADALINO,* R. D. PETRASSO,** P. B. RADHA, S. P. REGAN, F. H. SEGUIN,** W. SEKA, R. W. SHORT, A. SIMON, M. D. SKELDON, S. SKUPSKY, C. STOECKL, R. P. J. TOWN, M. D. WITTMAN, B. YAAKOBI, AND J. D. ZUEGEL

University of Rochester, Laboratory for Laser Energetics
250 East River Road, Rochester, NY 14623-1299

*State University of New York at Geneseo

**Massachusetts Institute of Technology
United States of America

ABSTRACT

The principal role of the Laboratory for Laser Energetics (LLE) is the development and validation of the direct-drive approach to inertial fusion. The LLE experimental and theoretical programs in support of this mission were organized to provide a moderate-gain option for the U.S. National Ignition Facility (NIF). Experimental implementation of the LLE program is carried out on the LLE's 30-kJ, 60-beam, UV OMEGA laser. This paper summarizes the status of the direct-drive ICF physics program at LLE with emphasis on the development of beam-smoothing techniques, long-scale-length plasma interaction experiments, direct-drive planar-foil hydrodynamic instability experiments, the effect of laser nonuniformity on target stability, integrated spherical target implosion experiments, design of direct-drive targets, development of target diagnostic techniques, and implementation of cryogenic-fuel-layering technology.

I. INTRODUCTION

Within the U.S. National ICF program, the principal role of the Laboratory for Laser Energetics (LLE) is the development and validation of the direct-drive approach to inertial fusion. The LLE experimental and theoretical programs in support of this mission are organized to provide a moderate-gain option for the National Ignition Facility (NIF). Experimental implementation of the LLE program is carried out on the LLE's 30-kJ, 60-beam, UV OMEGA laser in collaboration with Lawrence Livermore (LLNL) and the Los Alamos (LANL) National Laboratories.

This paper summarizes the status of the direct-drive ICF physics program at LLE with emphasis on the development of beam-smoothing techniques, long-scale-length plasma interaction experiments, direct-drive planar-foil hydrodynamic instability experiments, the effect of laser nonuniformity on target stability, integrated spherical target implosion experiments, design of direct-drive targets, development of target diagnostic techniques, and implementation of cryogenic-fuel-layering technology.

To provide the required irradiation uniformity for direct-drive ICF, we have developed and implemented on OMEGA two-dimensional smoothing by spectral dispersion (2-D SSD) [1]. The OMEGA SSD system is operating with a 2-D bandwidth of $1.25 \times 1.75 \text{ \AA}$. Using recently innovated technology for fabricating distributed phase plates (DPP's), the 2-D SSD system on OMEGA has demonstrated a single-beam nonuniformity of 12% rms, which corresponds to 4% rms for 60-beam irradiation of spherical targets. It is anticipated that the nonuniformity will be reduced to 2% rms for

a 2-D SSD bandwidth of $3 \times 10 \text{ \AA}$ in the IR (for modulation frequencies of 3 and 10 GHz, respectively) and with distributed polarization rotators (DPR's). The effectiveness of DPR's was demonstrated on five-beam planar Rayleigh–Taylor target experiments [2]. Efficient broad-bandwidth frequency conversion was demonstrated recently at LLE [3]. SSD has also been shown to decrease backscattered light in indirect-drive targets [4–9], and an SSD system is being implemented on the NIF with the ability not to preclude its 2-D enhancement for direct-drive experiments on the NIF.

Laser–plasma interactions were investigated in exploding-foil plasmas with density-gradient scale lengths comparable to those expected in direct-drive NIF coronal plasmas. The plasma was created by exploding CH foils with 18 OMEGA beams. The plasma was then heated with 20 additional OMEGA beams, creating a density-scale length of approximately 1 mm, a peak on-axis density of 18% of critical density, temperature in excess of 3.5 keV, and a velocity-gradient length of 1 mm. An interaction beam outfitted with various phase plates then permitted carrying out interaction experiments at 2×10^{14} , 6×10^{14} , and $1.5 \times 10^{15} \text{ W/cm}^2$ average intensity. The peak density was determined by stimulated Raman scattering (SRS) for the underdense plasma. No stimulated Brillouin scattering was observed in these experiments when phase plates (DPP's) were used. Similar experiments were carried out in plasmas generated from thick targets where a critical surface remains throughout the interaction time. Here, too, no SBS was observed when DPP's were used at $1.5 \times 10^{15} \text{ W/cm}^2$.

Hydrodynamic instabilities and laser imprinting experiments [2,10,11] have been carried out in planar as well as spherical geometries. Various beam-smoothing techniques were used including phase plates with no bandwidth, 2-D SSD, and DPR's. The imprinting was observed using face-on radiography after Rayleigh–Taylor growth, and it was clearly seen that the smallest level of laser imprinting corresponded to the best irradiation uniformity achieved with the use of SSD as well as DPR's [2]. Radiography was also used to measure the Rayleigh–Taylor growth rate in planar foils [12] accelerated at $100 \mu\text{m/ns}^2$ at a laser intensity of $2 \times 10^{14} \text{ W/cm}^2$. These foils had imposed mass perturbations with initial wavelengths of 20, 31, and 60 μm . The measured growth rates compare favorably with simulations carried out using the 2-D hydrodynamic code *ORCHID*.

In a spherical-target experiment designed to investigate hydrodynamic instabilities in a converging geometry [13–16], we have measured conditions in both the fuel and the pusher layers of imploding capsules. The RT growth during deceleration was measured using buried signature layers on the inside of the shell and Ar doping in the fuel. The signature layers were either CD or Ti-doped polymer layers buried 0 to 5 μm from the fuel–pusher interface. X-ray spectroscopy and monochromatic x-ray imaging were used to interrogate the signature layer [17–20].

The development of target diagnostics to characterize the extreme density and temperature conditions of ICF capsules is a high priority of the LLE program. An alternative to x-ray backlighting was developed whereby the cold, compressed shell can be imaged using $K\alpha$ line radiation in titanium-doped shell implosions [19,20]. By measuring the dimensions of the cold pusher shell at the time of peak compression and shell area density via K-edge absorption, it was possible to estimate the shell density.

Charged particles from fusion reactions are also used to measure core conditions. Using a novel charged-particle spectrometer [21,22] jointly developed with MIT, measurements have been made of the charged-particle spectra emitted during direct-drive shell implosions. In some of the initial experiments with this device the fuel ion temperature during the thermonuclear burn was determined by measuring the ratio between DD fusion reactions and D^3He reactions in D^3He -filled capsules. Various charged particle signatures are used to diagnose the core and shell areal densities.

To achieve high-density conditions of interest to NIF direct-drive capsules, a cryogenic capsule target filling, characterization, and handling system is being

constructed in a joint effort with General Atomics and LANL. This system will be completed in 1999 and used to carry out direct-drive validation experiments in preparation for direct-drive experiments on NIF.

II. ILLUMINATION UNIFORMITY

High laser-irradiation uniformity is an important requirement for successful direct-drive ICF. Direct-drive laser irradiation uniformity is achieved on OMEGA for different ranges of spatial frequencies by a number of techniques. The technique of smoothing by spectral dispersion (SSD) [1] significantly reduces irradiation nonuniformity at high spatial frequencies by rapidly shifting the laser speckle pattern generated by distributed phase plates (DPP's) [23,24]. A high-frequency electro-optic phase modulator produces a time-varying wavelength modulation that is subsequently angularly deflected by a diffraction grating required to shift the speckle pattern. Extremely smooth, time-averaged intensity profiles are achieved on a time scale corresponding to the inverse bandwidth impressed by the phase modulation. Two-dimensional SSD (2-D SSD) extends the smoothing benefits of SSD by combining the deflections of the laser speckle pattern in two orthogonal directions that are created by two separate stages of bulk electro-optic phase modulators.

The current 2-D SSD implementation on OMEGA employs phase modulators operating at 3.3 and 3.0 GHz in a single-pass configuration. It produces a maximum infrared bandwidth of $1.25 \times 1.75 \text{ \AA}$, which is frequency converted to a total ultraviolet bandwidth of approximately 0.25 THz (UV). FM-to-AM conversion mechanisms and phase modulator performance currently limit this maximum bandwidth.

The smoothing performance for the current 2-D SSD implementation, as well as a system planned to produce over 1 THz of bandwidth with a similar number of independent speckle patterns, is presented in Fig. 1, which plots the time-integrated rms irradiation nonuniformity on target versus integration time, including the effects of DPR's. The initial smoothing rate is directly proportional to the SSD bandwidth, while the asymptotic nonuniformity is inversely related to the square root of the number of independent speckle patterns on the target. For an SSD system employing critical dispersion, this roughly corresponds to the number of FM sidebands imposed by the phase modulator on the beam. The asymptotic uniformity for both systems is essentially the same, but the integration time required to achieve 2% nonuniformity is reduced from nearly 250 ps to about 70 ps by increasing the total SSD bandwidth. A useful review of various alternate approaches to beam smoothing is found in Ref. [25].

Achieving high beam uniformity on OMEGA requires both generation of large infrared bandwidths and efficient frequency conversion of these bandwidths into the ultraviolet. Bandwidth generation will soon be improved by implementing a double-pass, 2-D SSD architecture that is limited only by the efficiency of the current OMEGA frequency-conversion crystals to approximately 0.35 THz (UV). The double-pass architecture also incorporates a 10 GHz frequency phase modulator to reduce the

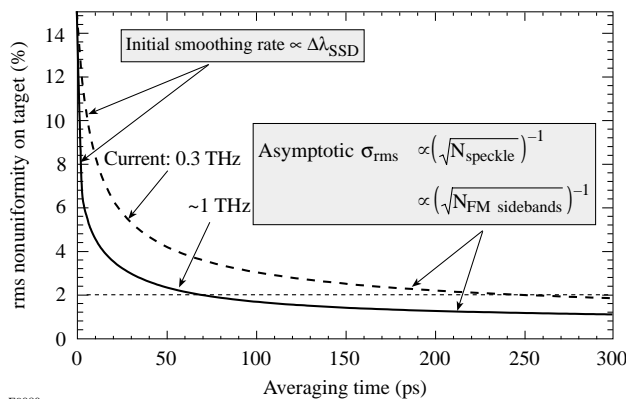


Fig. 1. Plot of time-integrated rms irradiation nonuniformity on target as a function of averaging time for the current 0.25 THz bandwidth SSD system on OMEGA (dashed curve) and that for the improved 1 THz SSD system.

smoothing time and will allow increasing the color cycles in the future to ultimately achieve 1-THz (UV) bandwidth. The ultimate configuration should achieve a 2-D SSD bandwidth of $1.5 \times 12 \text{ \AA}$ in the IR using phase modulators operating at 3.3 and 10 GHz, respectively. Approximately 2% rms irradiation nonuniformity on target is projected for this system within 60 ps.

Converting the infrared bandwidth corresponding to these UV bandwidths on OMEGA requires enhanced frequency conversion using a dual-tripler scheme [3] recently proposed at LLNL and demonstrated at LLE. Due to the expense and long procurement cycle for the additional tripler crystals, enhanced bandwidth conversion will be implemented first on 10 beams to perform planar geometry experiments and later on all 60 OMEGA beams for spherical implosion studies.

Polarization smoothing using distributed polarization rotators (DPR's) [2,25,26] effectively doubles the number of speckle patterns generated on target by each beam, resulting in a $\sqrt{2}$ reduction in nonuniformity for spatial frequencies above 12 mm^{-1} ($\lambda = 80\text{-}\mu\text{m}$ -wavelength). DPR's implemented on five OMEGA beams for planar Rayleigh–Taylor targets have already demonstrated the predicted smoothing improvements, and a full complement of DPR's have been ordered for OMEGA spherical implosion experiments and will be installed in 1999.

The temporal dependence of beam smoothing produced by SSD on OMEGA was investigated by recording ultraviolet equivalent-target-plane (ETP) images of 100-ps and 3-ns square laser pulses. An ETP image of a laser pulse with zero accumulated B -integral ($\Sigma B < 0.5$) was also recorded to quantify the amount of beam smoothing due to the beam self-phase modulation at high laser powers.

An ETP setup recorded the images with a charge-coupled-device (CCD) camera instead of film. The low noise level of the CCD camera is fully exploited in this experiment to extract power spectra with negligible noise levels. The power spectrum is the azimuthal sum at each frequency of the square of the Fourier amplitudes, and the cutoff wave number is given by the smallest laser speckle. The power spectra are normalized to the dc component, and the σ_{rms} is defined as the square root of the ratio of the power in the high frequencies to the power in the low frequencies (e.g., $k < 0.04 \mu\text{m}^{-1}$).

Power spectra calculated from the measured ETP images for various laser pulses are shown in Fig. 2. The power spectrum for $\Sigma B = 0$ and no FM bandwidth (top curve) has the highest $\sigma_{\text{rms}} = 0.94$ (designed value: $\sigma_{\text{rms}} = 0.99$). The second curve is the power spectrum of a 100-ps pulse without SSD and $\Sigma B = 5.0$ radians resulting in $\sigma_{\text{rms}} = 0.82$. The same pulse with SSD (0.25 THz, third curve) reduces σ_{rms} to 0.21. A 3-ns square pulse with SSD [0.25 THz, fourth (bottom) curve] yields $\sigma_{\text{rms}} = 0.06$. It should

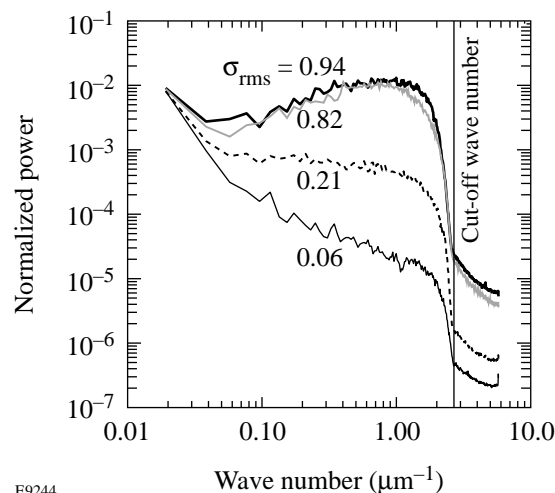


Fig. 2. Power spectra calculated from the measured ETP images for various laser pulses of the SSD smoothing time experiment.

be noted that a smoothing time of 3 ns is unrealistically long, but that smoothing times of 100 ps to 300 ps are more likely for direct-drive ICF experiments.

III. LONG-SCALE-LENGTH PLASMA PHYSICS EXPERIMENTS

The OMEGA geometry is well suited to carrying out planar-foil experiments designed to produce NIF-like plasma conditions. A large plasma is typically created by exploding a flat foil with a subset of OMEGA beams. The plasma is heated with additional beams to create a density-scale length of approximately 1 mm, a peak on-axis density of 18% of critical density ($n_e \approx 1.7 \times 10^{21} \text{ cm}^{-3}$), and temperatures in excess of 3.5 keV. Using an interaction beam focused with a specially designed phase plate, experiments can be carried out for intensities spanning the range of 10^{14} W/cm^2 to $1.5 \times 10^{15} \text{ W/cm}^2$ average intensity.

In one set of experiments designed to simulate NIF plasma conditions, solid targets were irradiated with stacked 1-ns square-top pulses to generate a drive pulse lasting approximately 3 ns. An interaction beam at an intensity of $1.5 \times 10^{15} \text{ W/cm}^2$ was focused into the critical density plasma. Observations of the backscattered light (see Fig. 3) indicate that there is no significant stimulated brillouin scattering present with an interaction beam smoothed by means of SSD.

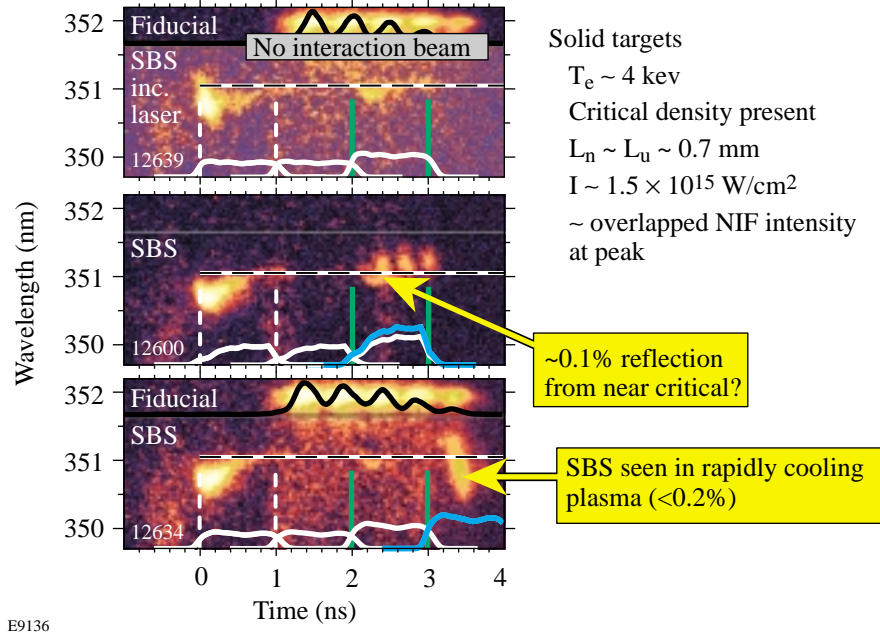


Fig. 3. Streak camera recordings of heating beams, interaction beam, and SBS backscatter in long-scale-length plasma experiments carried out on OMEGA. Shot 12639 is a control experiment with no interaction beam. On shot 12600 the interaction beam is timed to coincide with peak density conditions; on shot 12634, the interaction beam arrives after the heating beams have turned off. The highest reflection ($<0.2\%$) is observed when the interaction beam irradiates the rapidly cooling plasma after the heating beams are turned off.

IV. IMPRINTING MEASUREMENTS

We define laser beam imprinting to be the generation of mass perturbations seeded by laser nonuniformities. Planar-driven-foil experiments were conducted on OMEGA to investigate the effect of improved uniformity on imprinting and the related instability growth. The experimental setup for carrying out these measurements is shown in Fig. 4. The effect of improved uniformity is evident visually on the x-ray radiographs taken of the driven foils at 1.9 ns of a 3-ns pulse (see Fig. 5). With only phase plates (DPP's) significant nonuniformity is observed. With 2-D SSD (at 0.25 THz), and more so with distributed polarization rotators (DPR's), the nonuniformity is significantly

reduced. Fourier analysis of the target radiographs shows the beneficial effects of improved irradiation uniformity (see Fig. 6).

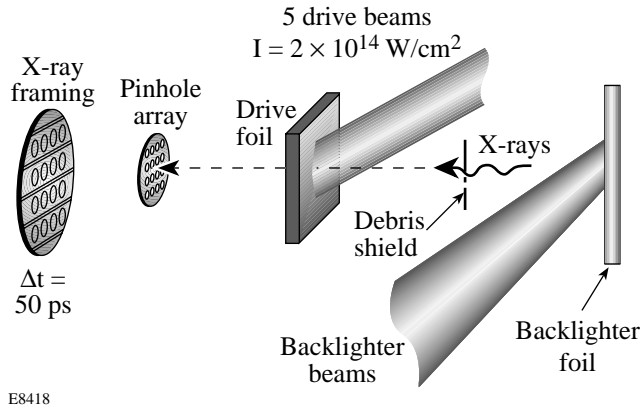
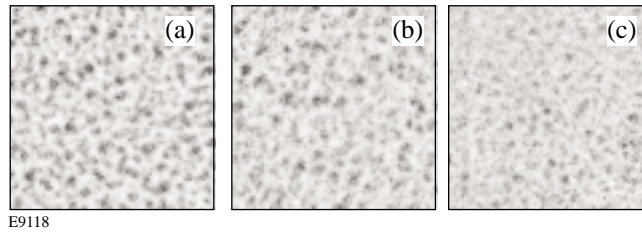


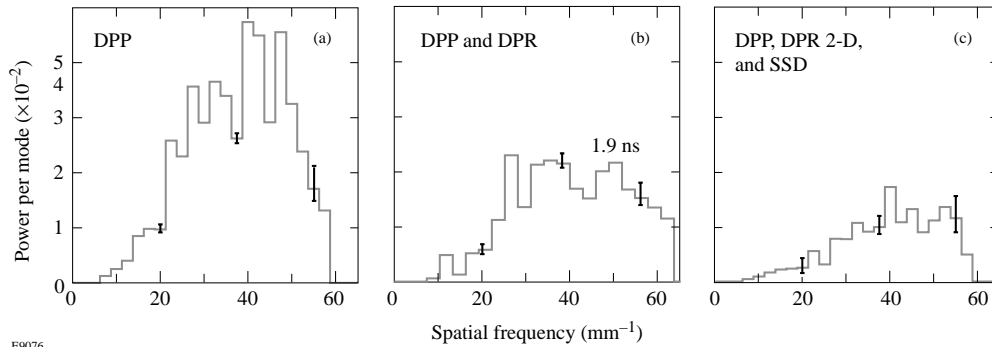
Fig. 4. Experimental set up for carrying out imprinting measurements on driven foils.

E8418



E9118

Fig. 5. The effect of increased uniformity is observed in x-ray radiographs of accelerated targets at 1.9 ns into a 3-ns pulse: (a) DPP only, (b) DPP and 2-D SSD, and (c) DPP and 2-D SSD and DPR's.



E9076

Fig. 6. Fourier analysis of target radiographs shows the beneficial effects of reduced irradiation nonuniformity.

V. SPHERICAL BURNTHROUGH TARGET EXPERIMENTS

A series of spherical burnthrough experiments were conducted to investigate the effects of laser uniformity changes on RT growth in imploding capsules [13–16]. These experiments used time-resolved x-ray spectroscopy to measure x-ray emission from a signature layer buried under a CH ablator (see Fig. 7). The onset time of x-ray line emission from this layer has been shown to be a sensitive indicator of both irradiation nonuniformities and Rayleigh–Taylor growth. Spectra were recorded from targets imploded using DPP-smoothed beams with and without SSD. Analysis of the data was carried out using a multimode RT postprocessor to the 1-D hydrocode *LILAC*, which

uses an initial perturbation spectrum derived from actual single-beam uniformity data [14]. The conversion between laser uniformity and initial mass perturbation (the “imprint parameter”) in the model is calculated by normalizing against one experimental point and is then left unchanged for all subsequent calculations. Figure 8 shows the measured and calculated signature-layer emission times (burnthrough times) as a function of CH ablator thickness. The effective SSD smoothing time can be inferred from this type of experiment.

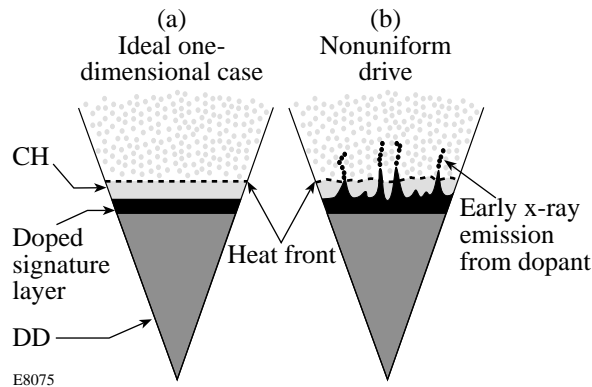


Fig. 7. Schematic of spherical burnthrough targets.

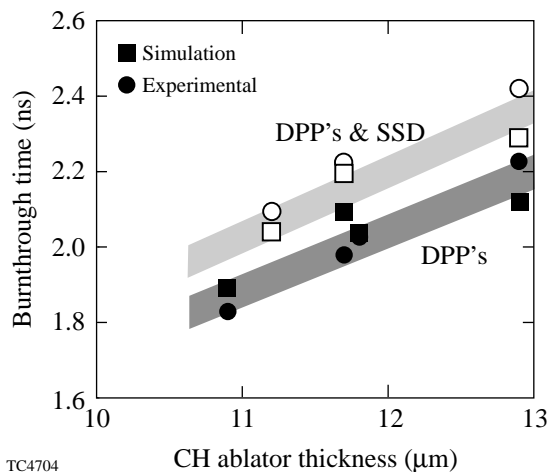


Fig. 8. Plot of measured (round points) and calculated burnthrough times (squares) as a function of CH ablator thickness for the cases with DPP's only and with full DPP's and SSD.

VI. DIAGNOSTICS FOR HIGH-DENSITY IMPLOSIONS

In a collaboration that includes scientists from LLE, MIT, and LLNL, two magnetic charged-particle spectrometers [21,22] (see Fig. 9) using an array of CR-39 track detectors were fielded on OMEGA. Spectroscopic measurements of energetic charged particles were carried out on OMEGA. Individual line profiles of charged fusion products were obtained, including $D-^3\text{He}$ protons (14.7 MeV) and alphas (3.6 MeV), DT alphas (3.5 MeV), and DD protons (3.0 MeV) and tritons (1.0 MeV). The measurements provided fusion yields, ion temperatures, fuel and ablator areal densities, and identification and quantification of anomalous charged-particle acceleration effects. In addition, energetic ablator ions with energy up to 1.2 MeV were observed. In particular, under certain conditions, sharply defined “lines” of energetic ablator protons were detected. When they occur, they have strong intensities at energies around 400 keV, with separations between adjacent “lines” of the order of 20 keV. These data were obtained with a spectrometer with a 7.6-kG magnet and CR-39 track detectors. The spectrometers resolve particles from 50 keV to 30 MeV (proton-equivalent energy, or energy of a particle with the same gyroradius as a proton of this energy).

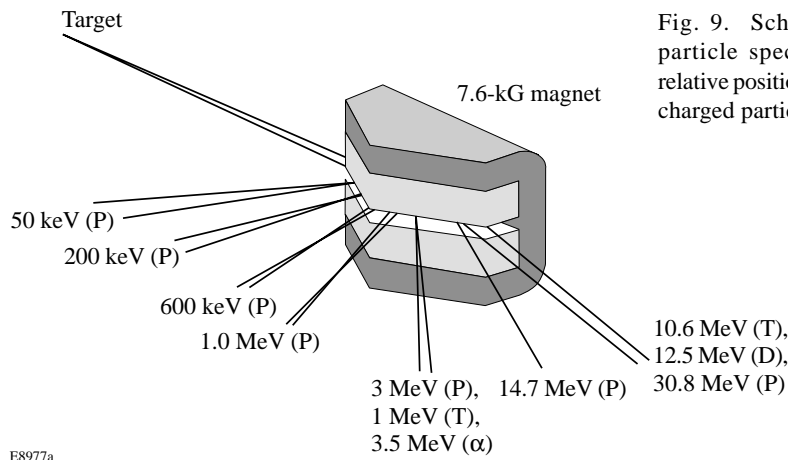


Fig. 9. Schematic of charged particle spectrometer showing relative positions of various energy charged particles.

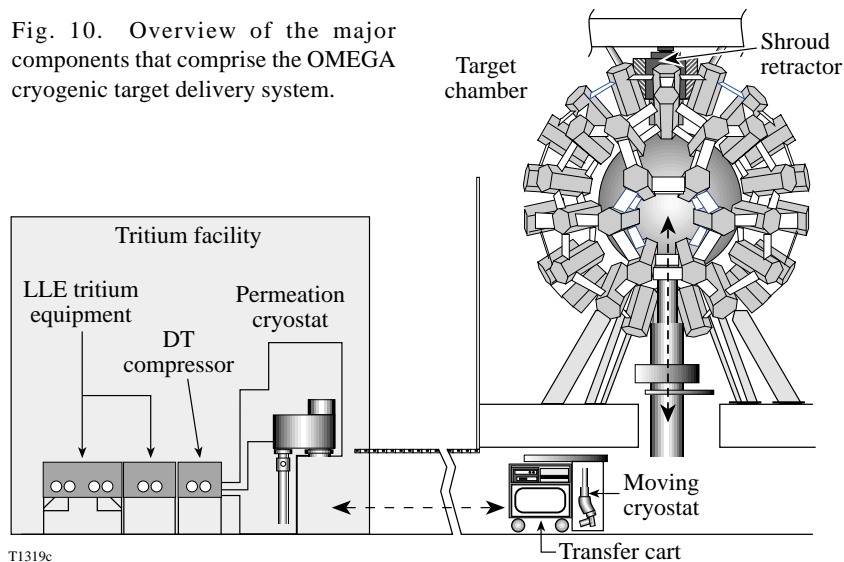
E8977a

VII. OMEGA CRYOGENIC-TARGET-HANDLING SYSTEM UPDATE

The design of the OMEGA Cryogenic-Target-Handling System (OCTHS) has been a 5-year collaborative project undertaken initially by General Atomic Corp. (GA) and assisted in recent years by LLE and LANL. The design phase is complete. Equipment has been procured and fabricated. Individual components are arriving from vendors. These components are being tested, in parallel, at GA and at LLE. The testing is planned to be completed at GA by March 1999, and all the equipment will be in-house at Rochester by April 1999. The system (see Fig. 10) will be integrated with the existing facility during the summer of 1999. The schedule is for the system to be operational with deuterium/helium mixtures by October 1999.

Direct-drive targets (1-mm-diam and $\leq 3\text{-}\mu\text{m}$ wall thickness) will be filled to a maximum room temperature pressure of 1500 atm (DT or D_2/He) and then cooled to 18 K. These conditions provide a $100\text{-}\mu\text{m}$ ice layer inside the target. Four targets can be processed simultaneously. Targets are individually transported to the center of the target chamber using a portable cryostat. Here the cooling shrouds are retracted (using a linear motor) at a constant acceleration of 2.5 g, which equates to a maximum velocity of 5 m/s. The frozen target is exposed to ambient room radiation for < 50 msec, before the laser is fired. During this time the target is calculated to increase in temperature by less than 0.3 K, thus maintaining its structural and material integrity.

Fig. 10. Overview of the major components that comprise the OMEGA cryogenic target delivery system.



T1319c

VIII. ACKNOWLEDGMENT

This work was supported by the U.S. Department of Energy Office of Inertial Confinement Fusion under Cooperative Agreement No. DE-FC03-92SF19460, the University of Rochester, and the New York State Energy Research and Development Authority. The support of DOE does not constitute an endorsement by DOE of the views expressed in this article.

IX. REFERENCES

1. SKUPSKY, S. *et al.*, Laser-beam pulse shaping using spectral beam deflection, *J. Appl. Phys.* **73** (1993) 2678–2685.
2. BOEHLY, T. R. *et al.*, The reduction of laser imprinting using polarization smoothing on a solid-state ICF laser, submitted to *J. Appl. Phys.*
3. EIMERL, D. *et al.*, Multicrystal designs for efficient third-harmonic generation, *Opt. Lett.* **22** (1997) 1208–1210; BABUSHKIN, A. *et al.*, Demonstration of the dual-tripler scheme for increased-bandwidth third-harmonic generation, *Opt. Lett.* **23** (1998) 927–929.
4. MOODY, J. D. *et al.*, Beam smoothing effects on the stimulated Brillouin scattering (SBS) instability in Nova exploding foil plasmas, *Phys. Plasmas* **2** (1995) 4285–4296.
5. MOODY, J. D. *et al.*, Beam smoothing effects on stimulated Raman and Brillouin backscattering in laser-produced plasmas, *J. Fusion Energy* **12** (1993) 323–330.
6. BALDIS, H. A. *et al.*, Parametric instabilities and laser-beam smoothing, Lawrence Livermore National Laboratory, Livermore, CA, ICF Quarterly Report UCRL-LR-105821-93-3 (1993) 137–144.
7. MACGOWAN, B. J. *et al.*, Laser–plasma interactions in ignition-scale hohlraum plasmas, *Phys. Plasmas* **3** (1996) 2029–2040.
8. MONTGOMERY, D. S. *et al.*, Effects of laser beam smoothing on stimulated Raman scattering in exploding foil plasmas, *Phys. Plasmas* **3** (1996) 1728–1736.
9. FERNÁNDEZ, J. C. *et al.*, Measurement of laser-plasma instability relevant to ignition hohlraums, *Phys. Plasmas* **4** (1997) 1849–1856.
10. BOEHLY, T. R. *et al.*, The effect of increased irradiation uniformity on imprinting by 351-nm laser light, in *Laser Interaction and Related Plasma Phenomena*, edited by MILEY, G. H. and CAMPBELL, E. M. (American Institute of Physics, New York, 1997), Vol. 406, pp. 122–129.
11. SMALYUK, V. A. *et al.*, Studies of the 3-D evolution of imprinting in planar targets accelerated by UV light, *Bull. Am. Phys. Soc.* **42** (1997) 1910–1911.
12. KNAUER, J. P. *et al.*, Single-mode Rayleigh-Taylor growth-rate measurements with the OMEGA laser system, in *Laser Interaction and Related Plasma Phenomena*, edited by MILEY, G. H. and CAMPBELL, E. M. (American Institute of Physics, New York, 1997), Vol. 406, pp. 284–293.
13. BRADLEY, D. K. *et al.*, Measurements of core and pusher conditions in surrogate capsule implosions on the OMEGA laser system, *Phys. Plasmas* **5** (1998) 1870–1879.
14. DELETTREZ, J. *et al.*, Effect of barrier layers in burnthrough experiments with 351-nm laser illumination, *Phys. Rev. A* **41** (1990) 5583–5593.
15. BRADLEY, D. K., DELETTREZ, J. A., AND VERDON, C. P., Measurements of the effect of laser beam smoothing on direct-drive inertial-confinement-fusion capsule implosions, *Phys. Rev. Lett.* **68** (1992) 2774–2777.
16. DELETTREZ, J., BRADLEY, D. K., AND VERDON, C. P., The role of the Rayleigh-Taylor instability in laser-driven burnthrough experiments, *Phys. Plasmas* **1** (1994) 2342–2349.

17. YAAKOBI, B. *et al.*, Novel methods for diagnosing mixing and laser-fusion target performance using x-ray spectroscopy of an embedded titanium layer, *Opt. Photonics News* (1997) 42–43.
18. MARSHALL, F. J. *et al.*, A high-resolution x-ray microscope for laser-driven planar-foil experiments, *Phys. Plasmas* **5** (1998) 1118–1124.
19. YAAKOBI, B. AND MARSHALL, F. J., Imaging the cold, compressed shell in laser implosions using the $K\alpha$ fluorescence of a titanium dopant, accepted for publication in *J. Quant. Spectrosc. Radiat. Transf.*
20. YAAKOBI, B., MARSHALL, F. J., AND BRADLEY, D. K., Pinhole-array x-ray spectrometer for laser-fusion experiments, accepted for publication in *Appl. Opt.*
21. PETRASSO, R. D. *et al.*, Measuring implosion symmetry and core conditions in the National Ignition Facility, *Phys. Rev. Lett.* **77** (1996) 2718–2721.
22. HICKS, D. G. *et al.*, Design of an electronic charged particle spectrometer to measure ρR on inertial fusion experiments, *Rev. Sci. Instrum.* **68** (1997) 589–592.
23. KESSLER, T. J. *et al.*, Laser phase conversion using continuous distributed phase plates, in *Solid State Lasers for Application to Inertial Confinement Fusion*, edited by ANDRÉ, M. L. (SPIE, Bellingham, WA, 1997), Vol. 3047, pp. 272–281.
24. LIN, Y., KESSLER, T. J., AND LAWRENCE, G. N., Distributed phase plates for super-Gaussian focal-plane irradiance profiles, *Opt. Lett.* **20** (1995) 764–766.
25. ROTHENBERG, J. E., Comparison of beam-smoothing methods for direct-drive inertial confinement fusion, *J. Opt. Soc. Am. B* **14** (1997) 1664–1671.
26. Phase conversion using distributed polarization rotation, Laboratory for Laser Energetics LLE Review **45**, NTIS document No. DOE/DP40200-149 (1990) 1–12. Copies may be obtained from the National Technical Information Service, Springfield, VA 22161.